nature communications

Article

https://doi.org/10.1038/s41467-024-52714-7

Enhanced *Staphylococcus aureus* protection by uncoupling of the α-toxin-ADAM10 interaction during murine neonatal vaccination

Received: 30 March 2023

Accepted: 19 September 2024

Published online: 08 October 2024

Check for updates

Kelly L. Tomaszewski[1,2,9], Meagan Blanchard[1,9], Reuben Olaniyi[1,6], Hannah R. Brenton[1], Samantha Hayes[1,7], Farheen Fatma[3], Gaya K. Amarasinghe[3], Byoung-Kyu Cho[4], Young Ah Goo[4], Andrea C. DeDent[5,8], Stephanie A. Fritz[1] & Juliane Bubeck Wardenburg[1,2]

Staphylococcus aureus remains a leading global cause of bacterial infection-associated mortality and has eluded prior vaccine development efforts. *S. aureus* α-toxin (Hla) is an essential virulence factor in disease, impairing the T cell response to infection. The anti-Hla antibody response is a correlate of human protective immunity. Here we observe that this response is limited early in human life and design a vaccine strategy to elicit immune protection against Hla in a neonatal mice. By targeted disruption of the interaction of Hla with its receptor ADAM10, we identify a vaccine antigen ($Hla_{H35L/R66C/E70C}$, Hla_{HRE}) that elicits an ~100-fold increase in the neutralizing anti-Hla response. Immunization with Hla_{HRE} enhances the T follicular helper (T_{FH}) cell response to *S. aureus* infection, correlating with the magnitude of the neutralizing anti-toxin response and disease protection. Furthermore, maternal Hla_{HRE} immunization confers protection to offspring. Together, these findings illuminate a path for *S. aureus* vaccine development at the maternal-infant interface.

Staphylococcus aureus infection results in over 1 million deaths globally per year[1]. While infection prevention is of public health importance, prior vaccine development efforts have failed[2]. Each candidate vaccine to reach clinical trials has been highly immunogenic as defined by the vaccine-elicited antibody response, however these responses were not defined as a correlate of human immunity against *S. aureus*. Further, recent studies have indicated that the pre-existing immune response to *S. aureus* that develops in the context of naturally occurring exposure throughout life may be detrimental to vaccine efficacy[3,4]. Novel approaches to vaccine development are needed, grounded in an understanding of human immunity and cognizant of the demand for a population-level solution.

S. aureus α-toxin (Hla) is a conserved pore-forming toxin required for disease pathogenesis[5]. Expressed by nearly all clinical isolates, Hla utilizes A Disintegrin and Metalloprotease 10 (ADAM10) as a cellular receptor to inflict host cell injury[6–10]. ADAM10 is a type I transmembrane protein that is widely expressed on human cells (Supplementary Fig. 1a). Characterized by an N-terminal metalloprotease domain,

[1]Department of Pediatrics, Washington University School of Medicine, St. Louis, MO, USA. [2]Forward Defense, LLC, St. Louis, MO, USA. [3]Department of Pathology and Immunology, Washington University School of Medicine, St. Louis, MO, USA. [4]Mass Spectrometry Technology Access Center at the McDonnell Genome Institute - Washington University School of Medicine, St. Louis, MO, USA. [5]Department of Microbiology, The University of Chicago, Chicago, IL, USA. [6]Present address: Merck & Co, West Point, PA, USA. [7]Present address: St. Jude Children's Research Hospital, Memphis, TN, USA. [8]Present address: Cleveland Clinic Innovations, Cleveland Clinic, Cleveland, OH, USA. [9]These authors contributed equally: Kelly L. Tomaszewski, Meagan Blanchard.
e-mail: jbubeck@wustl.edu

ADAM10 contributes to cellular and tissue development, homeostasis, and response to injury, dependent on proteolytic cleavage of ADAM10 substrates in a cell-type specific manner[11]. Extensive knowledge of both Hla and ADAM10 has enabled a detailed understanding of the molecular mechanisms by which the toxin-receptor interaction contributes to tissue injury in *S. aureus* infection. Upon binding of the Hla monomer to ADAM10, assembly of the heptameric toxin pore is initiated[6]. Pore formation on the host cell membrane results in the upregulation of the catalytic activity of ADAM10 and concomitant cleavage of native ADAM10 substrates, including E-cadherin, VE-cadherin, and platelet glycoprotein VI[6,7,9,12–14]. These cleavage events, together with cellular injury attributable to Hla pore formation, culminate in tissue-specific insults that are manifest in *S. aureus* disease.

Hla has emerged as a key target for vaccine development. Preclinical studies have revealed that active and passive immunization targeting Hla affords disease protection[15,16]. Among staphylococcal virulence factors, Hla is unique in its ability to impair the antigen-specific T cell response, promoting recurrent infection[17]. Neutralization of Hla leads to preservation of the T cell response in animal models[17], and enhances recovery of the T cell response following *S. aureus* infection in children[18]. The anti-Hla antibody titer is elevated among pediatric subjects who exhibit protection against recurrent infection[19], however a study by Wu et al., revealed that infants <1 year of age harbor a lower serum anti-Hla titer and neutralizing capacity than children 2–10 years of age[20]. Consistent with this finding, up to 50% of infants and children with *S. aureus* skin and soft tissue infection (SSTI) experience disease recurrence[21]. Together, these findings define the anti-Hla response as a correlate of human protective immunity, suggesting that elicitation of a highly neutralizing anti-Hla antibody response early in life is a strategic target for vaccine development. In this study, we characterize a fully detoxified structural variant of Hla as a vaccine antigen, and reveal the mechanism by which this antigen amplifies T cell-mediated protection against *S. aureus* disease early in life.

Results

Hla antigen screen to enhance the toxin-neutralizing vaccine response

To refine our knowledge of anti-Hla response development, we evaluated 343 subjects aged <1 to 18 years (Supplementary Table 1). Analysis of the anti-Hla titer by age revealed a gradual increase in the half-maximal effective concentration (EC50) over the first 5 years of life, with titers in children under 2 being most distinct from those of older children (Fig. 1a). Paired examination of the serum Hla neutralizing activity in a rabbit red cell (rRBC) protection assay confirmed that subjects <2 years exhibit response immaturity (Fig. 1b). *S. aureus* exposure through colonization is documented to occur in the first days and weeks of life, with mortality from *S. aureus* infection over the first 4 years of life rivaling that seen in older adults[1]. Together, these data suggest that the risk of both *S. aureus* disease and modification of the host response to this microbe occur early in life.

We, therefore, undertook a vaccine development approach designed to elicit immunity against *S. aureus* infection through neonatal vaccination. We hypothesized that the Hla-ADAM10 interaction and subsequent conformational changes that induce pore formation may influence vaccine efficacy. We generated a series of modified Hla antigens based on structural determinants and correlates of toxin function, in part based on the expected immunogenic properties derived from a combination of prior observations and T cell epitope prediction algorithms. Six distinct antigens were generated and evaluated including three full-length Hla variant antigens appended with a 6x-histidine tag to facilitate affinity purification (Supplementary Fig. 1b): Hla_{H35L} (purple) has been extensively studied as a toxoid vaccine that binds ADAM10 yet fails to form a stable pore[6,7,22], $Hla_{D45A/Y118F}$ (orange), predicted to interfere with β-barrel stem domain unfolding[23], and $Hla_{R66C/E70C}$ (blue), which abrogates cell binding[24]. We also examined a panel of peptide antigens (Supplementary Fig. 1c): Hla_{50}, harboring five tandem arrays of the first 50 amino acids of Hla that elicit protective immunity in animal models[25]; Hla_{P1}, a synthetic antigen harboring five tandem arrays of the immune epitope database-predicted T cell epitope Hla_{36-50}; and Hla_{P2}, a synthetic antigen harboring three distinct predicted T cell epitopes from Hla (Hla_{36-50}, Hla_{51-65}, and $Hla_{161-175}$). Each antigen was screened by delivery to groups of mice to examine vaccine efficacy compared to Freund's adjuvant control. Upon a screening subcutaneous challenge with *S. aureus*, mice receiving Hla_{H35L}, $Hla_{D45A/Y118F}$, and $Hla_{R66C/E70C}$ vaccines exhibited protection against abscess formation and dermonecrosis (Supplementary Fig. 1d). In contrast, mice receiving peptide vaccines exhibited similar or larger lesions than those observed in sham-vaccinated mice.

To further examine vaccine properties of the three full-length antigens, $Hla_{D45A/Y118F}$ and $Hla_{R66C/E70C}$ were modified to incorporate the H35L mutation to ensure full detoxification, which was verified in a rabbit red cell lysis assay (Supplementary Fig. 1e, Hla_{H35L} denoted Hla_H, $Hla_{H35L/D45A/Y118F}$ denoted Hla_{HDY}, and $Hla_{H35L/R66C/E70C}$ denoted Hla_{HRE}). As an initial functional immunologic screen, we delivered each candidate antigen to mice in a prime-boost regimen formulated with Freund's adjuvant. We confirmed that each candidate antigen

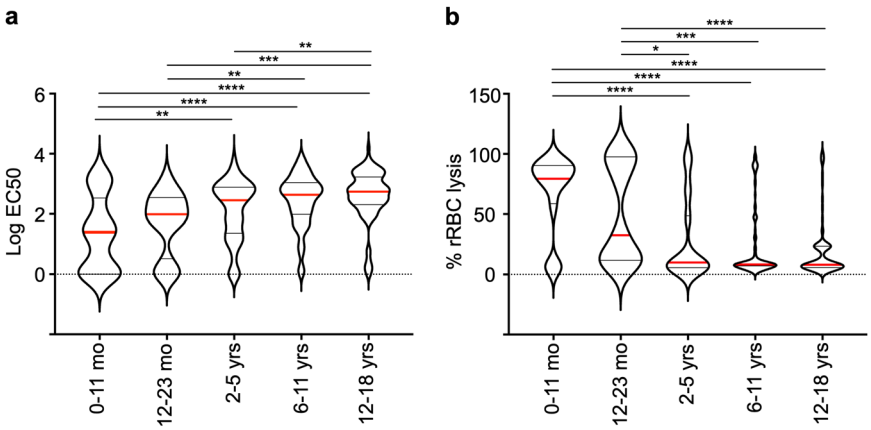

Fig. 1 | The neutralizing anti-Hla response is a vaccine target early in life. a Half-maximal effective concentration of anti-Hla reactive antibodies in sera from children within the designated age groups (Log EC50). **b** Serum-based protection against Hla-mediated (2 nM) rRBC lysis. Protection noted as percent compared to toxin-only control. For **a**, **b**, 75th and 25th (black) and 50th (red) percentiles noted. Data were analyzed by one-way ANOVA with Tukey's multiple comparisons test. $^{*}p < 0.05$, $^{**}p < 0.01$, $^{***}p < 0.001$, $^{****}p < 0.0001$. Source data are provided as a Source Data file.

https://doi.org/10.1038/s41467-024-52714-7

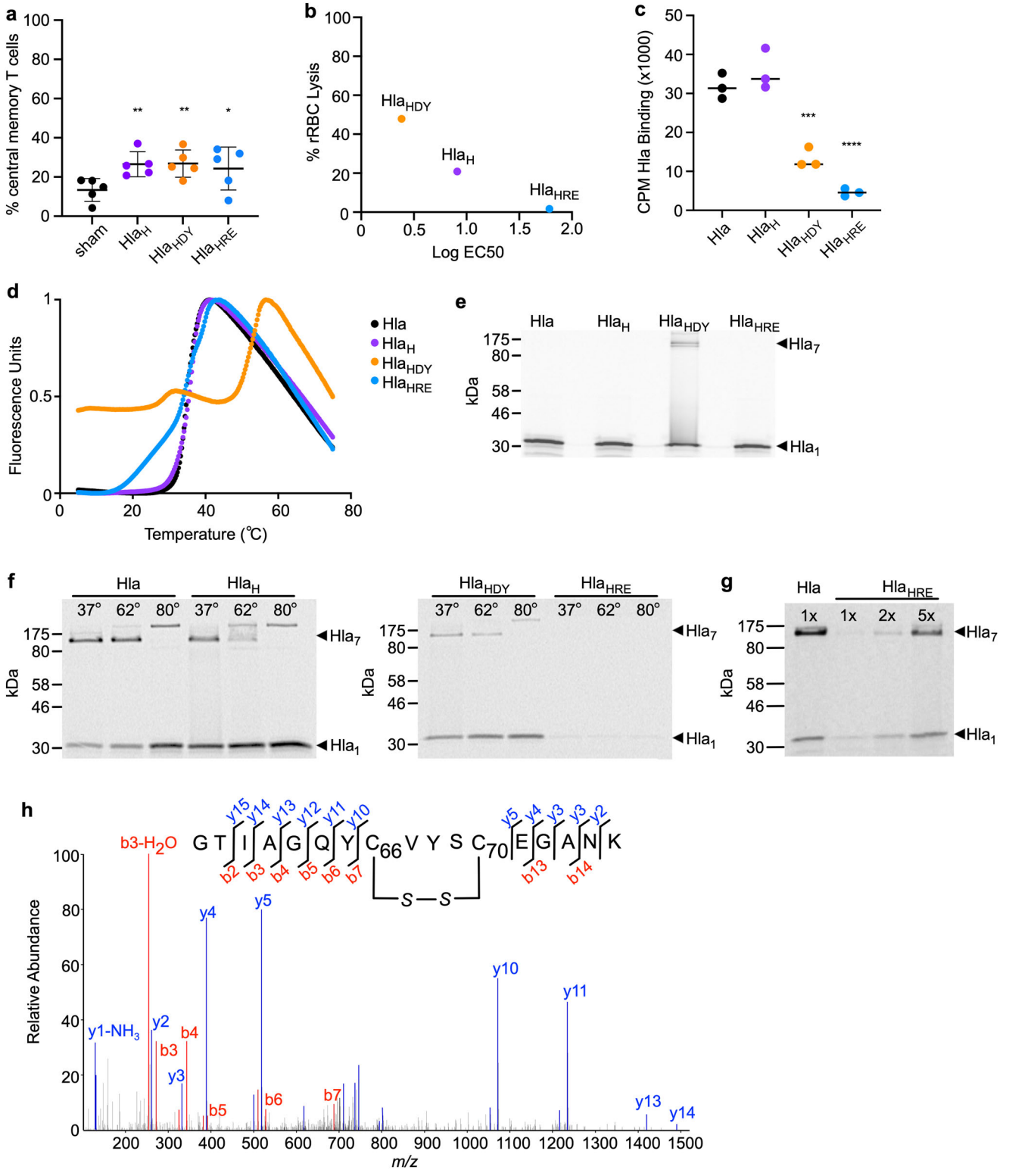

enhanced the antigen-specific memory T cell response to infection utilizing the ovalbumin-specific OT-II T cell system and an ovalbumin-expressing *S. aureus* strain (Fig. 2a)[17]. To assess the B cell response to immunization, we defined the serum toxin-neutralizing capacity in a rabbit red blood cell (rRBC) lysis protection assay and quantified the half-maximal anti-Hla titer (EC50) in serum from vaccinated mice. The vaccine-elicited antibody response varied in an antigen-specific manner, with Hla_{HRE} eliciting a high degree of toxin neutralization (Fig. 2b). These findings suggested that nearly identical antigens based on primary sequence can exhibit distinct biological properties that modify antigenicity and host immune response.

To characterize the biochemical properties of candidate antigens, we evaluated ADAM10 binding in a sensitive rRBC binding assay. Hla_H exhibited preservation of binding compared to wild-type Hla, with diminution of Hla_{HDY} binding and near-complete loss of Hla_{HRE} binding (Fig. 2c). Melt curve analysis of each antigen revealed that the Hla_{HDY}

Fig. 2 | Analysis of Hla-targeting vaccine candidate antigens. a OT-II CD4$^+$ T cell subset analysis of OT-II CD4$^+$ T cells harvested from the draining lymph nodes of mice immunized with adjuvant alone (sham) or candidate Hla vaccines Hla_H, Hla_{HDY}, Hla_{HRE}. Tissue harvest occurred 7 days following subcutaneous infection with 1×10^8 CFU of wild-type *S. aureus* USA300/LAC strain compared by non-parametric one-way ANOVA with Dunnette's multiple comparisons test. Data represents biological replicates ($n = 5$ per group) with mean ± SD. **b** Correlation between protection against rRBC lysis upon treatment with 2 nM Hla and serologic anti-Hla titer (Log EC50) from mice following immunization with Hla_{H35L} (purple), Hla_{HDY} (orange), Hla_{HRE} (blue). Data represents the mean of biological replicates ($n = 5$) **c** Vaccine antigen Hla variant binding to rRBC as compared to wild-type Hla by non-parametric one-way ANOVA with Tukey's multiple comparisons test, Hla_{HDY} $p = 0.0005$, Hla_{HRE} $p < 0.0001$. Data represents the median of technical replicates ($n = 3$ per group). **d** Melting curve analysis of Hla_H, Hla_{HDY}, and Hla_{HRE} compared to wild-type Hla. **e** SDS-PAGE analysis of ^{35}S-methionine labeled Hla, Hla_H, Hla_{HDY}, and Hla_{HRE} produced by coupled in vitro transcription and translation. **f** Analysis of heptamer assembly and stability for Hla, Hla_H, Hla_{HDY}, and Hla_{HRE}, evaluated following incubation of radiolabeled toxin with rRBCs for one hour at room temperature followed by incubation at 37, 62, or 80 °C for 10 min. **g** Analysis of Hla_{HRE} heptamer capability with increasing concentrations of radiolabeled toxin. The radiolabeled toxin was incubated with rRBCs for one hour at room temperature, followed by incubation at 37 °C. Relative densitometric units of monomeric and heptameric toxin was quantified using ImageJ software. SDS-PAGE separation was followed by phosphor-image detection of labeled toxin; for **e**–**g**, toxin monomers (Hla_1) and oligomers (Hla_7) are noted. **h** Disulfide bond identified in antigen Hla_{HRE} by mass spectrometry. Disulfide bond (S-S) peptide linking of Cys66 and Cys70 within the Hla_{HRE} protein was identified by LC-MS/MS analysis and validated by manual alignment of y or b-ion matching. *$p < 0.05$, **$p < 0.01$, ***$p < 0.001$, ****$p < 0.0001$. Source data are provided as a Source Data file.

variant is structurally distinct from Hla, Hla_H, and Hla_{HRE} (Fig. 2d). This finding was confirmed by SDS-PAGE analysis where the Hla_{HDY} variant formed the oligomeric toxin (Hla_7) in solution without exposure to a cell membrane (Fig. 2e), while wild-type Hla and other variants were present solely in monomeric form (Hla_1). Examining the biological properties of these Hla variants on rRBCs, we observed that the wild-type Hla oligomer exhibits temperature stability up to 62 °C (Fig. 2f, left), illuminating the functional defect in the Hla_H variant that is unable to form a temperature-stable oligomer (Fig. 2f, left). Hla_{HDY} retains the ability to oligomerize on the cell membrane proportionate to its binding capability (Fig. 2f, right), whereas the Hla_{HRE} variant exhibited limited monomer binding and oligomer formation (Fig. 2f, right). To assess the oligomerization efficiency of Hla_{HRE} on the rRBC surface, we examined increasing concentrations of Hla_{HRE} until achieving an equivalent amount of monomeric Hla rRBC binding (Fig. 2g). Densitometric quantification of the oligomer:monomer ratio revealed a 3.6:1 ratio for Hla compared to 1.9:1 ratio for Hla_{HRE} signifying a functional oligomerization defect in addition to the binding defect observed in the Hla_{HRE} antigen. As Hla undergoes an ordered series of intramolecular movements upon binding to enable heptameric pore formation, we hypothesized that this defect in functional oligomerization of Hla_{HRE} may represent a broader conformational restriction of this antigen based on the incorporation of two cysteine residues that may contribute to disulfide bond formation. To examine whether Hla_{HRE} has a disulfide bond between C66 and C70, we subjected the antigen to mass spectrometry-based analysis, which revealed that the majority of purified Hla_{HRE} does indeed incorporate an intramolecular disulfide bond (Fig. 2h).

Protective efficacy of the Hla_{HRE} candidate vaccine antigen

We sought to evaluate each antigen's protective efficacy in a prime-boost neonatal vaccination model (Fig. 3a), recognizing that neonates and infants represent the vaccine-targetable population in which to enhance the anti-Hla response in humans (Fig. 1). Several immunologic challenges arise in vaccine design for the neonatal population[26,27]. The neonatal immune response is characterized by delayed formation of the germinal center (GC) with a resultant decrease in the quantity and quality of the affinity-matured antibody response[28]. Moreover, an increased frequency of FoxP3$^+$ T regulatory (T_{REG}) cells in neonates, together with the presence of maternally-derived antibodies that can modulate vaccine antigen availability and presentation, amplifies the challenge of vaccine formulation for this population[28]. We thus performed an initial survey of each candidate antigen formulated with four adjuvants: Alum (Alhydrogel), AddaS03 (AS03-like), MPLA+Alum (AS04-like), and CpG-ODN1585. This array of adjuvants was selected for initial studies owing to their distinct immunostimulatory properties, reasoning that a broad-based approach to vaccine formulation would enable us to specifically evaluate the relevance of antigenic variation. To rigorously examine vaccine protection, we utilized a high inoculum of *S. aureus* (1×10^8 CFU) to elicit primary SSTI in 5–6-week-old mice with a secondary challenge performed on the contralateral flank 21 days following the primary infection (Fig. 3a). All antigens elicited protection against primary abscess formation (Fig. 3b, left) and dermonecrosis (Fig. 3b, right) when formulated with Alum. Upon recurrent infection, Hla_{HRE} elicited protection against abscess formation and dermonecrosis (Fig. 3c), while Hla_H and Hla_{HDY} vaccines afforded limited protection. The diminution of vaccine-mediated protection was prominent for Hla_H (76.9 ± 9.3% to 28.4 ± 11%) and Hla_{HDY} (76.1 ± 13% to 11.5 ± 4.6%) compared to that observed for Hla_{HRE} (94.4 ± 2.6% to 76.5 ± 8.3%). Enhanced protective immunity was observed with the Hla_{HRE} vaccine candidate during secondary infection irrespective of the adjuvant utilized (Supplementary Fig. 2, AddaS03 (a), MPLA + Alum (b), CpG-ODN1585 (c)). Analysis of the anti-Hla neutralizing antibody titer in serum from each group of vaccinated mice prior to primary infection revealed a marked benefit in those mice receiving the Hla_{HRE} antigen irrespective of adjuvant (Fig. 3d). Correlation analysis of the serologic anti-Hla antibody response and toxin-neutralizing activity from each group of immunized mice reflected the importance of the vaccine antigen as the principal determinant of vaccine-mediated protection, as the Hla_{HRE} vaccine elicited an increased anti-toxin-neutralizing antibody response within each adjuvant group compared to the Hla_H vaccine (Fig. 3e, Alum, 92.3-fold; AddaS03, 23.8-fold; MPLA+Alum, 84.2-fold; CpG-ODN1585, 14.6-fold).

Hla_{HRE} augments the germinal center response to vaccination

Amplification of the neutralizing antibody response suggested that the Hla_{HRE} antigen promotes affinity maturation of the antibody response. Affinity maturation is the product of the germinal center (GC) response, characterized by a dynamic interaction between antigen-presenting cells, B cells, and antigen-specific T cells within the draining lymph node (dLN)[29]. While T cell activation is required to initiate the vaccine response, differentiated antigen-specific T follicular helper (T_{FH}) cells are essential for affinity-based positive selection of GC B cells[30]. CXCR5 upregulation in a subset of activated T cells within the interfollicular (or mantle) zone of the dLN enables T cell migration to the nascent GC and subsequent upregulation of Bcl6, the lineage-defining transcription factor of T_{FH} cells[31]. The essential role of the T_{FH} compartment in B cell maturation in the GC is evident in Bcl6 knockout mice which are devoid of GCs, thereby unable to generate a mature antibody response[32]. To evaluate whether the GC response distinguishes the Hla_H and Hla_{HRE} antigens, we first examined the kinetics of the developing anti-Hla neutralizing response to vaccination. Owing to blood volume and tissue limitations in neonatal mice, we subjected 5-week-old mice to prime-boost vaccine delivery with each antigen adjuvanted with Alum. As early as 1-week post-boost, a significant increase in the Hla-neutralizing antibody response was elicited by Hla_{HRE} relative to that of Hla_H, $p < 0.0001$ (Fig. 4a). By 3 weeks post-

https://doi.org/10.1038/s41467-024-52714-7

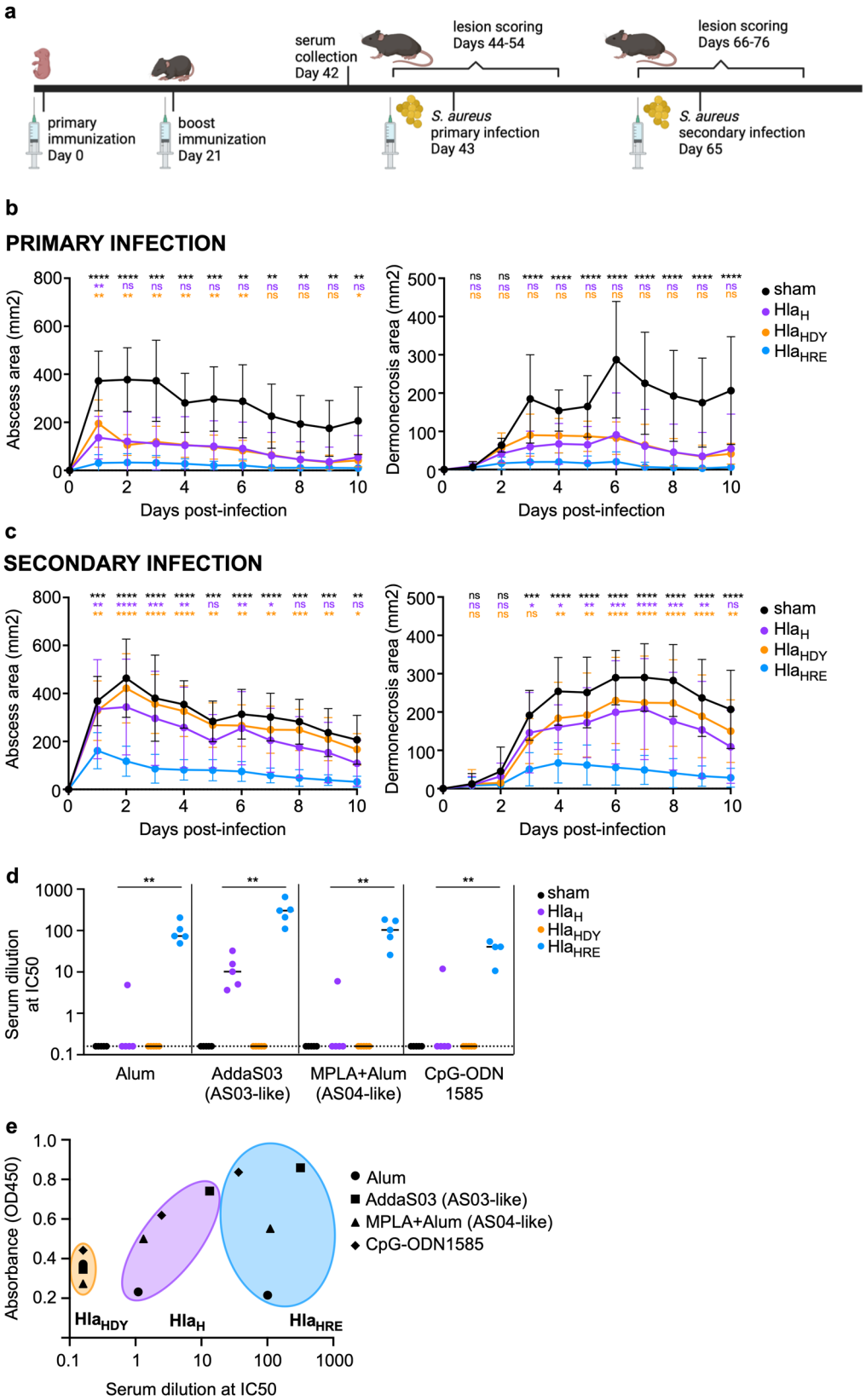

boost when the elicited antibody response is expected to be fully matured, an increase in the neutralizing antibody titer was seen for both Hla_H and Hla_{HRE} antigens, however, the Hla_H-elicited response remained lower in magnitude than that of the Hla_{HRE} response, $p = 0.0002$ (Fig. 4a). The functional attributes of these elicited antibodies were evaluated by assessing blockade of radiolabelled Hla binding (Fig. 4b) and oligomerization (Fig. 4c) on rabbit red cells. In both studies, Hla_{HRE}-elicited antibodies exhibited enhanced performance compared to those elicited by Hla_H ($p = 0.0002$ and $p = 0.004$, respectively).

We extended these studies to directly evaluate the cellular response within the vaccine-draining iliac lymph node response at day 7

Fig. 3 | Neonatal vaccination model demonstrates protection against *S. aureus* skin and soft tissue infection. a Schematic showing the timeline of neonatal vaccination and SSTI modeling (BioRender). Skin abscess (left) and dermonecrosis (right) area following primary (**b**) ($n = 10$ per group) and re-infection (**c**) of immunized mice ($n = 10$ for sham and Hla_H, and $n = 9$ for Hla_{HDY} and Hla_{HRE}) with 1×10^8 CFU *S. aureus*, noting the statistical significance of Hla_{HRE} compared to each vaccine condition designated by color. Data analyzed by two-way ANOVA with Tukey's multiple comparisons test, mean ± SD. Independent experiments were repeated twice. **d** Serum dilution from mice in (**b**, **c**) that affords 50% protection against rRBC lysis (IC50) when exposed to 0.8 pM recombinant Hla, noting the statistical significance of Hla_{HRE} compared to Hla_H by one-way ANOVA with Tukey's multiple comparisons test. Data represents the median of biological replicates, $n = 5$ per group for all antigen-adjuvant combinations, except $n = 4$ for CpG-ODN1585 Hla_{HRE}. **e** Correlation between serum dilution that affords 50% protection against Hla-mediated (0.8 pM) rRBC lysis and anti-Hla titer from mice following immunization. Data represents the mean from biological replicates in (**d**). Independent experiments were repeated twice. $^*p < 0.05$, $^{**}p < 0.01$, $^{***}p < 0.001$, $^{****}p < 0.0001$. Source data are provided as a Source Data file. Figure 3a Created with BioRender.com released under a Creative Commons Attribution-NonCommercial-NoDerivs 4.0 International license.

following prime-boost vaccination with either Hla_H or Hla_{HRE}. We did not observe differences in either the total population of $CD19^+$ GC B cells marked by co-expression of GL7/Fas (Fig. 4d and Supplementary Fig. 3a) or the proliferating ($Ki67^+$) $CD19^+GL7^+Fas^+$ B cells (Fig. 4e and Supplementary Fig. 3a). Similarly, no significant difference was observed in the total $CD4^+$ T cell compartment between the two vaccines (Fig. 4f and Supplementary Fig. 3b). In contrast, we observed an increase in median CXCR5 fluorescence intensity in the bulk $CD4^+$ population, $p = 0.0143$ (Fig. 4g and Supplementary Fig. 3b) and $Ki67^+$ $CD4^+$ cells, $p = 0.032$ (Fig. 4h and Supplementary Fig. 3b) in Hla_{HRE}-immunized mice. As CXCR5 expression is required for early T_{FH} differentiation to render these cells capable of migration to the nascent germinal center, this finding suggests that the Hla_{HRE} antigen amplifies the pre-T_{FH} response.

We hypothesized that vaccine-mediated protection by Hla_{HRE} would elicit an enhanced T_{FH} response to infection. We thus examined the $CXCR5^+$ compartment in the dLN of vaccinated mice 7 days following secondary *S. aureus* SSTI (as in Fig. 3). Following infection, clinical lesions remained prominent in the sham and Hla_H vaccinated mice, however, were limited in the Hla_{HRE} vaccine recipients (Fig. 4i). As the T_{FH} population is relatively rare in the dLN, we first utilized mass cytometry to analyze pooled dLN to gate on $CXCR5^+$ cells that co-express ICOS and PD1, revealing an increase in the $CD4^+$ $CXCR5^+$ $ICOS^+$ $PD1^+$ T_{FH} compartment in Hla_{HRE}-vaccinated mice relative to that in Hla_H-vaccinated mice (Supplementary Fig. 4a). Recent studies have illustrated that the GC T_{FH} compartment is differentiated from the pre-T_{FH} population by high-level expression of CXCR5 and Bcl6 in response to infection[31,33,34]. To enhance the specificity of our analysis, we utilized a flow cytometric approach to detect $CXCR5^{hi}$ $Bcl6^{hi}$ $CD4^+$ T cells in individual dLN harvested following *S. aureus* infection (Supplementary Fig. 3c). Compared to sham and Hla_H vaccinated mice, animals receiving Hla_{HRE} exhibited expansion of the proliferating $CD4^+$ $CXCR5^{hi}$ $Bcl6^{hi}$ T_{FH} population, $p = 0.0012$ and $p = 0.0033$, respectively (Fig. 4j).

We then examined whether the beneficial effects of Hla_{HRE} vaccination reflected the role of Hla in the modulation of the T cell compartment. While our prior studies revealed that Hla blunted the antigen-specific T cell response[17], these studies did not encompass the evaluation of the functional specificity of the T cell response. Groups of mice were infected with wild-type *S. aureus* or its isogenic Δ*hla* variant and dLN subjected to mass cytometry 7 days post-primary infection. Deletion of Hla was associated with an increase in the $CXCR5^+$ $ICOS^+$ $PD1^+$ T_{FH} population (Supplementary Fig. 4b). Analysis of individual mice infected with WT *S. aureus*, Δ*hla*, and the Δ*hla* variant complemented with a plasmid that enables restoration of Hla expression (Δ*hla*::p*hla*) confirmed that Hla expression negatively impacts the $CXCR5^{hi}$ $Bcl6^{hi}$ GC T_{FH} population, WT vs Δ*hla* $p = 0.0326$, Δ*hla vs* Δ*hla*::p*hla* $p = 0.0236$ (Fig. 4k).

Hla_{HRE} efficacy is preserved in the setting of prior antigen exposure

There is an increasing appreciation in the *S. aureus* field that vaccine failures may, in part, result from vaccine delivery to a non-naive host that harbors a pre-existing immune response that becomes amplified by vaccination[3,4]. We thus addressed the protective efficacy of the Hla_{HRE} vaccine in two clinical contexts in which pre-existing immunity is relevant: passive transfer of maternal antibodies that may limit vaccine antigen bioavailability and/or antigenicity[35], and in the setting of prior *S. aureus* infection. We first examined whether Hla_{HRE}-immunized dams conferred protection against *S. aureus* infection to their offspring (Fig. 5a). Pups from Hla_{HRE}-immunized dams exhibited protection against skin abscess and dermonecrosis (Fig. 5b, blue) compared to offspring of Alum-immunized dams (black), reflecting the neutralizing anti-Hla response (Fig. 5c). To evaluate whether passive transfer of maternal antibodies impaired the protective response to subsequent infant vaccination[35], we examined whether circulating anti-Hla antibodies in offspring adversely influenced the clinical outcome of active vaccination. Pups from sham (gray) and Hla_{HRE}-immunized (green) dams received Hla_{HRE} vaccination followed by *S. aureus* infection. Both groups manifest protection against *S. aureus* infection, as observed in pups born to mice that received passive immunity from maternal immunization (blue), suggesting that prior maternal immunity does not impair the functional outcome of active immunization. We extended these maternal-infant studies by evaluating the duration of the serologic response in offspring, recognizing that passively transferred antibodies are reported to exist in murine offspring up to ~15 weeks of life. Mice from each of the vaccine groups were sampled at 6, 8, 10, and 16 weeks of life and assessed for serum Hla-neutralizing properties. We observed a robust passive transfer of anti-Hla neutralizing function, consistent with the observed protection following maternal immunization (Supplementary Fig. 5, blue). Active immunization of pups following maternal Hla_{HRE} immunization (green) was indistinguishable from that observed in Hla_{HRE}-vaccinated pups born to dams that received sham vaccination with alum alone (gray), signifying that exposure to maternal anti-Hla antibody does not incur functional loss of the Hla_{HRE} vaccine response in offspring. A progressive decrease in the neutralizing antibody titer occurred in all groups over 10–16 weeks, as expected based on known kinetics of the vaccine response (Supplementary Fig. 5). We were unable to examine the duration of clinical protection against *S. aureus* infection in mice that were 16 weeks old owing to inter-mouse heterogeneity in the hair follicle cycle which directly effects re-epithelialization in response to injury[36].

To directly evaluate whether prior *S. aureus* infection modulated the protective efficacy of Hla_{HRE} vaccination, groups of naive 5-week-old mice were subjected to *S. aureus* SSTI followed by a prime-boost vaccine regimen with Alum alone or Alum-adjuvanted Hla_{HRE} vaccines (Fig. 5d). Hla_{HRE} conferred near-complete protection against infection on the contralateral flank two weeks following boost (Fig. 5e), reflecting the neutralizing anti-Hla response (Fig. 5f). Together, these findings suggest that vaccination with the Hla_{HRE} antigenic variant may not be as susceptible to the deleterious impact of pre-existing immunity on vaccine outcomes. It remains to be determined if this property reflects the biochemical nature of the Hla_{HRE} antigen itself, the specificity of the elicited antibody response, or is simply related to an antibody response generated against a secreted protein antigen.

T_{FH} amplification correlates with Hla_{HRE}-mediated protection

To understand the potential scope of clinical applicability of the Hla_{HRE} vaccine, we assessed protective efficacy in a series of distinct biological

https://doi.org/10.1038/s41467-024-52714-7

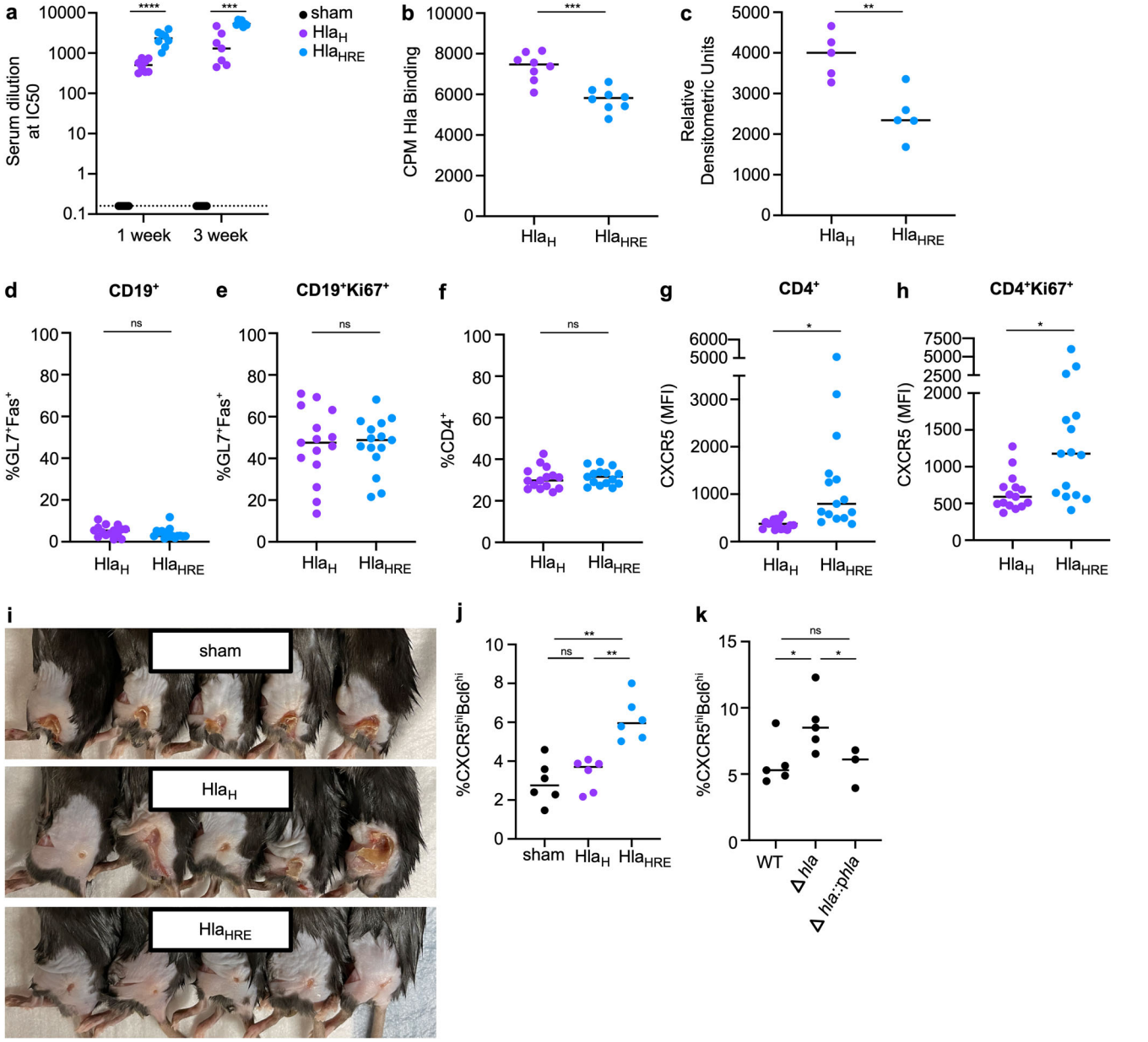

Fig. 4 | Hla$_{HRE}$ amplifies the T$_{FH}$ response. a Serum dilution from immunized mice that affords 50% protection against rRBC lysis (IC50) by 0.8 pM Hla, noting statistical significance of Hla$_{HRE}$ versus Hla$_H$ by two-tailed unpaired *t*-test. Data represents the median of biological replicates (1 week, $n = 8$/group, 3 weeks, $n = 7$/group). **b** Serum neutralization of Hla binding to rRBC comparing sera from mice in (**a**), noting statistical analysis by two-tailed unpaired *t*-test. Data represented as the median of biological samples ($n = 8$) represented as the mean of two technical replicates/samples. **c** Densitometric analysis of Hla oligomer formation on rRBC comparing immunized sera from mice in (**a**). Data represents the median of biological replicates ($n = 5$/group), analyzed by a two-tailed unpaired *t*-test. Analysis of left inguinal germinal center cells 1-week following immunization of mice with Hla$_H$ ($n = 15$) or Hla$_{HRE}$ ($n = 15$) comparing: **d** GL7$^+$Fas$^+$ B cells, **e** Ki67$^+$GL7$^+$Fas$^+$ B cells, **f** CD4$^+$ T cells, **g** CXCR5 median fluorescence intensity (MFI) on CD4$^+$ T cells, and **h** CXCR5 median fluorescence intensity (MFI) on CD4$^+$Ki67$^+$ T cells. Data represents the median of biological replicates, analyzed by a two-tailed paired *t*-test. **i** Gross pathology of skin lesions (2 days post-infection) in mice vaccinated as neonates with sham, Hla$_H$, or Hla$_{HRE}$ ($n = 5$). Analysis of CXCR5^{hi}Bcl6^{hi} in Ki67^{++}T$_{FH}$ cell compartment in mice in (**i**), data represents the median of biological replicates ($n = 6$). **k** Analysis of CXCR5^{hi}Bcl6^{hi} T$_{FH}$ cell compartment in mice subjected to primary infection with wild-type (WT) ($n = 6$), Δ*hla* ($n = 6$), or Δ*hla*::p*hla* ($n = 3$) variants of *S. aureus*. Statistical analysis by paired, two-tailed *t*-tests (**d**–**h**) and two-way ANOVA with Tukey's multiple comparisons test (**j**, **k**) $^*p < 0.05$, $^{**}p < 0.01$, $^{***}p < 0.001$, $^{****}p < 0.0001$. Source data are provided as a Source Data file.

settings. *S. aureus* skin infection is commonly modeled in male mice owing to both the epidermal structure of the skin, which facilitates histopathologic analysis, and the magnitude of the lesional differences that result from male hormone-mediated enhancement in *S. aureus* virulence[37]. We first demonstrated Hla$_{HRE}$ vaccine efficacy in protecting female mice against severe SSTI following neonatal vaccination (Supplementary Fig. 6a), consistent with the elicitation of the anti-Hla neutralizing antibody response (Supplementary Fig. 6b). Second, we evaluated protective efficacy in young mice that were not exposed to vaccination as neonates. Groups of 3-week-old naive mice received a priming immunization with either Alum alone or Alum-adjuvanted Hla$_{HRE}$ followed by a boost 14 days later (Supplementary Fig. 6c). When subjected to primary *S. aureus* infection, Hla$_{HRE}$-vaccinated mice exhibited protection from infection (Supplementary Fig. 6d), also reflecting a productive neutralizing anti-Hla antibody response (Supplementary Fig. 6e) and corresponding vaccine-elicited T$_{FH}$ response

https://doi.org/10.1038/s41467-024-52714-7

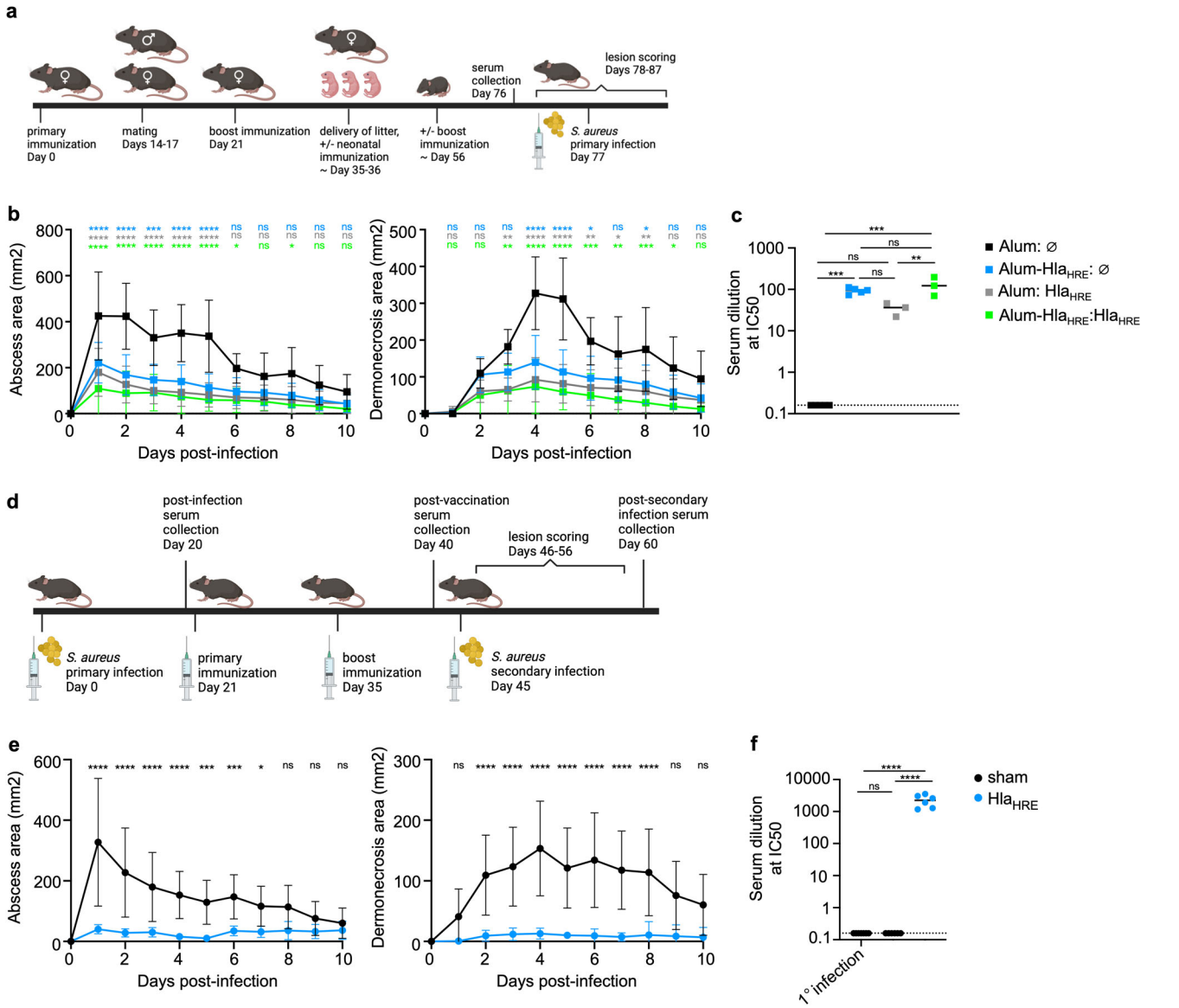

Fig. 5 | Hla$_{HRE}$ vaccine exhibits protective efficacy following maternal immunization and prior *S. aureus* exposure. a Schematic showing the timeline for maternal and neonatal vaccination followed by SSTI. **b** Skin abscess (left) and dermonecrosis (right) area of mice following primary infection with 1×10^8 CFU *S. aureus*. Mice were born to dams that received Alum or the Alum-Hla$_{HRE}$ vaccine; pups were either unimmunized (black $n = 4$ and blue $n = 8$, respectively), Alum immunized (gray, $n = 5$), or Alum-Hla$_{HRE}$ immunized (green, $n = 5$), noting statistical significance of Alum maternal immunization compared to each vaccine condition designated by color by two-way ANOVA with Tukey's multiple comparisons test. Data represented as the mean ± SD. **c** Serum dilution from mice in (**b**), that affords 50% protection against rRBC lysis (IC50) when exposed to 0.8 pM Hla. Statistical analysis by one-way ANOVA with Tukey's multiple comparisons test. Data represents the median of biological replicates (black $n = 5$, blue $n = 5$, gray $n = 3$, and green $n = 3$). **d** Schematic showing the timeline for a model in which juvenile mice are exposed to *S. aureus* infection prior to vaccination. **e** Skin abscess (left) and dermonecrosis (right) area of mice (sham $n = 13$, Hla$_{HRE}$ $n = 14$) following secondary infection with 1×10^8 CFU *S. aureus*. Data represents mean ± SD, analyzed by two-way ANOVA with Sidak's multiple comparisons test. **f** Serum dilution from mice in (**e**), that affords 50% protection against rRBC lysis (IC50) when exposed to 0.8 pM Hla. Data represents the median, analzyed by one-way ANOVA with Tukey's multiple comparisons test (primary infection group $n = 7$, sham $n = 6$, and Hla$_{HRE}$ $n = 6$). Source data are provided as a Source Data file. Figure 5a, d Created with BioRender.com released under a Creative Commons Attribution-NonCommercial-NoDerivs 4.0 International license.

(Supplementary Fig. 6f). Finally, we evaluated whether a non-tagged variant of the Hla$_{HRE}$ antigen was functional. Neonatal vaccination with both the tagged Hla$_{HRE}$ antigen and the native, untagged Hla$_{HRE}$ antigen (Hla$_{HRE\text{-}NATIVE}$) elicited significant protection against *S. aureus* skin infection (Supplementary Fig. 6g). While a minor improvement in the clinical efficacy of Hla$_{HRE\text{-}NATIVE}$ was observed early in the course of infection, the neutralizing IC50 was nearly identical for both antigens (Supplementary Fig. 6h).

Successful vaccine design, evaluation, and implementation in the human population requires both antigen optimization and knowledge of the mechanism by which distinct adjuvants amplify desired host immune responses. We therefore assessed whether the observed adjuvant-specific differences (Alum, AddaS03, MPLA + Alum, and CpG-ODN1585) in potency of Hla$_{HRE}$ vaccine-mediated protection (Fig. 3 and Supplemental Fig. 2) reflected the magnitude of the T_{FH} response in the dLN. Evaluating the relationship between T_{FH} recovery from the dLN and clinical abscess size, we observed an inverse correlation (Fig. 6a). In accord with this finding, we observed a direct correlation between the IC50 of the neutralizing anti-Hla response and T_{FH} response (Fig. 6b). Together, these findings underscore the importance of the T_{FH} response as an immune correlate of protective efficacy of the Hla$_{HRE}$ vaccine, and suggests that

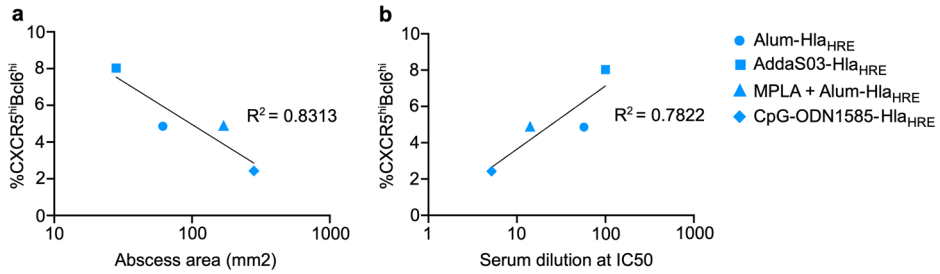

Fig. 6 | Hla_{HRE} vaccine formulation influences the T_{FH} response. a Inverse correlation of T_{FH} cell recovery and clinical abscess size from immunized mice after *S. aureus* SSTI infection. **b** Direct correlation between the anti-Hla neutralizing IC50 and T_{FH} response from immunized mice after *S. aureus* SSTI infection. All mice were subjected to priming immunization as neonates with a boost at the time of weaning. Data represents the mean of biological replicates ($n = 7$ per group for T_{FH} cell analysis and Alum-Hla_{HRE} $n = 11$, AddaS03-Hla_{HRE} $n = 10$, and $n = 12$ for MPLA +Alum-Hla_{HRE} and CpG-ODN1585-Hla_{HRE} groups). Data and R^2 values were analyzed by non-linear regression, semi-log line. Source data are provided as a Source Data file.

the magnitude of this response can be favorably modulated by vaccine formulation.

Discussion

Our findings in this study leverage the observation that the anti-Hla response is a defined correlate of human protective immunity to *S. aureus* in the pediatric population[19]. Through population-level analysis characterizing the development of anti-Hla response in childhood, we define a specific window of opportunity in the first two years of life to augment this response through vaccination. We describe a candidate Hla antigen, Hla_{HRE}, distinguished by its ability to elicit a robust toxin-neutralizing response. When delivered as a pre-exposure vaccination of neonatal mice or in a maternal vaccine strategy, Hla_{HRE} affords pre-clinical protection from severe *S. aureus* skin infection. Moreover, we have demonstrated that prior exposure to Hla is not an a priori limitation to successful amplification of the host immune response to the Hla_{HRE} vaccine. An analysis of the mechanism of protective immunity elicited by Hla_{HRE} revealed the importance of the T_{FH} response as a functional immunologic correlate of Hla_{HRE} vaccine-mediated protection.

These studies address several critical challenges within the *S. aureus* vaccine field. It has been recognized that vaccine development to target *S. aureus* has suffered from a lack of understanding of the T cell response to this pathogen. Consequently, vaccines have not been designed to elicit T cell-specific correlates of immune protection[38]. For the first time, we propose and evaluate a vaccine specifically designed to protect the T cell response to *S. aureus* early in life. Hla neutralization contributes to the protection of the antigen-specific T cell response during infection[17,18], thus providing mechanistic insight into the observed pre-clinical efficacy of the Hla_{HRE} vaccine. Detoxified Hla variants (including Hla_{H35L}, $Hla_{H35L/H48L}$) have previously been considered or are being evaluated for vaccine development[39]. Our studies illustrate that the specific antigenic form of Hla influences the magnitude of the neutralizing antibody response, revealing that some Hla variants may only generate modest vaccine protection. While it is possible that this response difference may be overcome by delivery of higher quantities of antigen or alternatively through booster regimens, the potency of the Hla_{HRE} antigen in amplification of the host immune response may be advantageous to enable antigen sparing and in settings such as the neonate and the elderly where the vaccine-elicited response may be limited by inherent attributes of host immunity.

As *S. aureus* is a leading cause of bacterial infection-associated mortality worldwide in the first year of life[1], our findings establish the scientific rationale for considering maternal immunization and/or neonatal Hla_{HRE} vaccination. Maternal immunization offers the attractive opportunity to afford protection of neonates against disease and modulation of the T cell response to *S. aureus* by Hla prior to the ability of active immunization to engender protection. As passive immunity will predictably wane, a durable approach to active immunization of the infant/child will be required to ensure long-term protection of the T cell response against this pathogen. It will be important to rely upon analysis of the epidemiology of *S. aureus* disease to inform ongoing vaccine development for this population.

At present, the precise molecular mechanism by which the Hla_{HRE} antigen amplifies the T_{FH} response to promote affinity maturation of anti-Hla antibody response is not fully understood. The increase in CXCR5 expression on pre-T_{FH} $CD4^+$ T cells following delivery of Hla_{HRE} compared with that observed upon Hla_H immunization suggests that Hla_{HRE} may more effectively promote a cDC2-dependent response, favoring T_{FH} differentiation[40]. While it was unexpected that two amino acid substitutions in Hla_{HRE} relative to Hla_H would alter the outcome of vaccination, a precedent for this level of antigen specificity in defining the host response to vaccination was observed in respiratory syncytial virus (RSV) vaccine development. Utilization of a pre-fusion-locked F antigen conformation elicits a highly neutralizing anti-viral antibody relative to that observed with post-fusion F antigen[41,42]. These two vaccine examples illustrate the exquisite specificity of antigen recognition by the host immune system, and indicate that a detailed analysis of antigen trafficking kinetics, cellular uptake and presentation, and duration of antigen availability in the GC will be required to fully elucidate the biological differences that underlie antigen specificity observed with the Hla_{HRE} variant. As Hla_H and Hla_{HRE} are functionally distinguished by ADAM10 binding capability, it will also be of interest to understand whether cellular trafficking of the Hla-ADAM10 complex on both professional and non-professional antigen-presenting cells modulates antigen distribution and processing.

Our findings have important implications for *S. aureus* vaccine development. Hla_{HRE}-elicited protective immunity is robust upon formulation with multiple distinct adjuvants (Fig. 3 and Supplemental Fig. 2), compelling the inclusion of this specific antigenic variant of Hla to optimize vaccination outcomes. Whether Hla_{HRE} is considered for use in a monovalent context or in the presence of other vaccine antigens, its biological properties are expected to augment the Hla-neutralizing antibody response. The use of Hla_{HRE} may simultaneously enhance the functional T cell and GC response to other antigens, especially as this antigen augments the T_{FH} response. Our studies, for the first time, indicate that the T_{FH} response is a key target of Hla in *S. aureus* pathogenesis. It is of interest to note that in recurrent human *Streptococcus pyogenes* (group A Strep) infection, modulation of the T_{FH} response has been implicated as a principal mechanism of immunoevasion[33]. While the T_{FH} response during *S. aureus* infection can be rigorously examined in modeling systems, it will be essential to translate these studies to human immunity to *S. aureus* in order to inform vaccine development. Variation in the magnitude of the T_{FH} response as a function of the adjuvant utilized (Fig. 6) indicates that it

may be possible to tailor the vaccine formulation to the target population of interest, simultaneously providing a framework on which to evaluate novel adjuvants to further optimize vaccine performance.

Together, these studies underscore the importance of Hla neutralization by a *S. aureus* vaccine. As a toxin that interferes with the development of T cell-mediated immunity to *S. aureus*[17], Hla neutralization is expected to not only protect against toxin-mediated cellular injury in disease, but, perhaps more importantly, ensure that the T cell compartment remains viable and poised throughout life to support the generation of a diverse immune response to the pathogen. Delivery of an Hla_{HRE}-containing vaccine early in life may thus afford protection against *S. aureus* infection in infants and children, but also enable the success of *S. aureus* vaccines developed for administration later in life to protect against disease-specific virulence factors. The Hla_{HRE} vaccine may thereby represent an opportunity to advance the development of a population-level *S. aureus* vaccine.

Methods

Study approval

All experimental procedures and reagents were approved by Washington University in St. Louis Institutional Biosafety Committee (protocol 14083). All animals in this study were housed according to Washington University in St. Louis IACUC guidelines, (ventilation sufficient to maintain appropriate temperature (68–79 °F) and humidity (30–70%) ranges and to control odor; standard diurnal light cycle 12-h light: 12-h dark) and all experimental procedures were approved by the IACUC of Washington University in St. Louis (protocol 22-0377). The collection and use of human samples in this study was approved by the University of Chicago Institutional Review Board. Written informed consent was obtained for all participants, with assent obtained from children of a developmentally appropriate age (~7 years of age or older). Schematic figures were created with BioRender and licensed for use in publication.

Participant population and sample and data collection

Participants were children 18 years and younger undergoing sedated procedures or imaging studies at Comer Children's Hospital. Upon enrollment, study personnel collected swab samples (CultureSwab Liquid Stuart, Becton Dickinson, Franklin Lakes, NJ) from the anterior nares, axillae, and inguinal folds of each participant to determine *S. aureus* colonization status via culture-based methods. Participants or their parents/legal guardians were asked to complete a survey regarding the subject's current and past medical history, and history of *S. aureus* infection or known skin and soft tissue infection in the participant or a household member. Lastly, serum samples were obtained from each participant. Samples were de-identified and stored in a secure repository at −80 °C. Gender was not considered in this study, which aimed to broadly classify the serologic response to *S. aureus* based on age without any other discriminatory or stratifying features of the subject population.

ELISA and antibody neutralization assays

Human serum analysis. Nunc Maxisorp 384-well plates (Fisher Scientific) were coated with Hla_{H35L} at 1 μg/ml in PBS and incubated overnight at 4 °C. Plates were blocked with 0.1% bovine serum albumin (BSA) in PBS for 2 h at room temperature. Patient sera samples were diluted 1:10 and then twofold for a total of 24 dilutions and transferred to the 384 Maxisorp plates for 1 h at room temperature. Plates were washed three times with PBS/0.05% Tween-20 and incubated with goat anti-human HRP conjugated antibody (Southern Biotech) at a 1:20,000 dilution for 1 h at room temperature. Plates were washed three times and developed for 30 min at room temperature with QuantaBlu Fluorogenic Peroxidase Substrate Kit, and reactions were stopped with QuantaBlu Stop Solution. Fluorometric detection was measured using a Tecan Infinite M200 Pro plate reader at excitation 320 nm and emission 400 nm. For the neutralization assay, patient sera samples were diluted 1:10 in 0.1% BSA/PBS and incubated with purified toxin for 1 h at room temperature. After incubation, 5×10^7 of prewashed rRBCs were added and incubated for 1 h at room temperature on a platform shaker. The final concentration of toxin for the assays was 2 nM. Cells were pelleted, and supernatant absorbance readings (450 nm) were used to generate non-linear regression curves with log (inhibitor) vs. response−variable slope curves using GraphPad Prism software.

Juvenile murine serum analysis. Sera was diluted 1:25 and then by fourfold serial dilutions for eight dilutions total. Anti-Hla titers were determined by ELISA as previously described and ELISA absorbance readings (450 nm) used for generation of four-parameter log(dose)-response curves using Prism software. For the neutralization assay, serum was diluted 1:100 and then twofold for eight dilutions total. The diluted serum was incubated with 2 nM purified toxin for 15 min at room temperature before 5×10^7 rRBCs were added then incubated at room temperature for 1 h. Cells and debris were pelleted, and supernatant absorbance readings (450 nm, Tecan Infinite M200 Pro) were used to generate non-linear regression curves with log (inhibitor) vs. response−variable slope curves using GraphPad Prism software. Both the ELISA and neutralization assays were performed in triplicate.

Neonatal murine serum analysis. 384-well Maxisorp plates (Thermo Fisher) were coated with 50 μL of 1 μg/mL Hla_{H35L} and incubated overnight at 4 °C. Plates were blocked with 0.1% BSA in PBS for 2 h at room temperature, following incubation with 15 μL of neonatal pre-infection sera for 2 h at room temperature. Plates were washed three times with PBS/0.05% Tween-20 and then incubated with 15 μL of goat anti-mouse IgG-HRP antibody (Southern Biotech) at a 1:20,000 dilution for 1 h at room temperature. Plates were washed three times and developed for 15 min at room temperature with 20 μL of TMB substrate kit (Thermo Scientific Pierce PI34021), and the reaction stopped with 20 μL of 2 N sulfuric acid (Fisher Scientific). Absorbance values were read at 450 nm using a Tecan Infinite M200 Pro plate reader. For neutralization assays, neonatal pre-infection sera was diluted twofold for a total of 16 dilutions and incubated for 1 h at room temperature with 0.8 pM purified Hla. After incubation, 30 μL of prewashed rabbit red cells (1×10^7 total cells) was added to the toxin/sera and incubated for 1 h at room temperature in a v-bottom 384-well plate (Thomas Scientific). Cells and debris were pelleted, and supernatant absorbance readings (450 nm, Tecan Infinite M200 Pro) were used to generate non-linear regression curves with log (inhibitor) vs. response−variable slope curves using GraphPad Prism software.

Adult murine serum analysis with high-dose immunization. Sera was collected 1 week, 2 weeks, and 3 weeks post prime and boost 20 μg vaccinations. Sera was diluted 1:4 in PBS, and assays were performed as described above.

Plasmid construction and Hla antigen purification

Toxin variants were cloned into the pET24b expression vector containing a C-terminal polyhistidine tag. Hla_{H35L} was previously generated as described[7]. $Hla_{D45A/Y118F}$ was generated via site-directed mutagenesis with template DNA from a pET24b construct containing wild-type Hla cDNA previously generated. The following oligos were utilized: D45A sense – 5′ GTATTTTATAGTTTTATCGATGCTAAAAATC ACAATAAAA 3′; D45A antisense – 5′ TTTTATTGTGATTTTTAGCATC GATAAAACTATAAAATAC 3′; Y118F sense – 5′ GTATATGAGTAC TTTAACTTTTGGATTCAACGGTAATGTTA 3′; Y118F antisense – 5′ TAA CATTACCGTTGAATCCAAAAGTTAAAGTACTCATATAC 3′. HlaR66C/E70C was previously generated in the Bubeck Wardenburg lab as a GST fusion protein in pGEX6P1. To generate a polyhistidine-tagged protein, template DNA from the pGEX6P1 construct containing R66C/E70C

cDNA was used with primers for restriction site cloning using XbaI and XhoI (New England Biolabs) into pET24b vector.

The following primers were used: sense – 5′ CGGCGGCTCGAG ATTTGTCATTTCTTCTTT 3′;

antisense – 5′ CGGCGGTCTAGAAGGAGGATATATATGGCAGATT CTGATATAATATT 3′.

Site-directed mutagenesis was used to incorporate the H35L mutation in $Hla_{D45/Y118F}$ and $Hla_{R66C/E70C}$ constructs with the following primers: sense – 5′

CTTATGATAAAGAAAATGGCATGCTCAAAAAAGTATTTTATAGTT TTATCGATG 3′;

antisense –5′ CATCGATAAAACTATAAAATACTTTTTTGAGCATGC CATTTTCTTTATCATAAG 3′. Mutagenesis reactions were DpnI (New England Biolabs) digested and transformed into *Escherichia coli* DH5α on selection agar. Each construct was sequenced (Azenta Life Sciences) for verification. Confirmed clones were then transformed into *E. coli* BL21 for recombinant protein expression and purification.

Peptide sequences Hla_{50}, Hla_{P1} and Hla_{P2} constructs were generated by SynBio Technologies, and constructs transformed into BL21 for protein expression and purification. Recombinant toxin variants were purified using standard protocols described previously, LPS extracted and evaluated by 10% SDS-PAGE followed by Coomassie blue staining.

Characterization assays for Hla antigens

Hemolysis assay. Rabbit red blood cell (rRBC) hemolysis was assayed by incubation of rRBCs (Hemostat Labs) with purified toxin variants ranging from 0.08 to 10 μg/mL for 1 h at room temperature. Following incubation, cells were pelleted by centrifugation, and supernatant absorbance at 450 nm was measured using a Tecan Infinite M200 Pro plate reader. Percent rRBC hemolysis were calculated relative to 1% Triton X-100 maximal lysis controls. The assays were performed in triplicate and repeated for reproducibility on separate days.

Radiolabeled toxin binding and oligomerization assay. Hla was synthesized by in vitro transcription and translation in an *E. coli* S30 extract (Promega) supplemented with T7 RNA polymerase, rifampin (rifampicin), and [^{35}S] methionine according to the manufacturer's instructions. For the binding assay, 125 μL of 12.5% rabbit red blood cells (rRBC) in K-PBSA/βME (20 mM potassium phosphate [monobasic], 150 mM NaCl pH 7.4, 1 mg/ml bovine serum albumin, 1 mM β-mercaptoethanol) was incubated with 10 μl of radiolabeled Hla mixture diluted 1:10 (~1 nM) for 5 min at room temperature. Cells were pelleted, washed twice with ice-cold PBS, resuspended in 200 μl of PBS, and added to scintillation fluid (Research Products International, Econo-Safe). Radioactivity from cell-bound toxin was quantified on a Beckman LS6000 scintillation counter. For oligomerization assays, rRBCs and radiolabelled Hla were used as described above for 1 h at room temperature. Following incubation, cells were pelleted and washed with 500 μl K-PBSA/βME and then resuspended in 90 μl 1× Laemmli buffer. Samples were divided into 30 μl aliquots and incubated at 37, 62, and 80 °C for 10 min before samples were loaded onto 10% sodium dodecyl sulfate (SDS)-PAGE gels for electrophoresis. The gels were dried, and results were visualized using a phosphorimager (GE Healthcare Typhoon Trio Imager). To analyze Hla_{HRE} oligomerization capability, rRBCs were treated as described above with 10 μl of increasing concentration of radiolabeled Hla mixture (1x = ~1 nM; 2x = ~2 nM, and 5x = ~5 nM) and incubated at 37 °C before samples were separated by SDS-PAGE and prepared as above. For binding and oligomerization assays using vaccinated mouse sera, each sera sample was diluted 1:5 in PBS, then incubated with 10 μl of radiolabeled Hla diluted 1:10 for 10 min at room temperature before adding the rabbit red cells. Assays were performed as described above. Binding assays were performed in triplicate and repeated for reproducibility on separate days. Oligomerization assays were performed with a single replicate and repeated for reproducibility on separate days.

Proteomics disulfide bond analysis of Hla_{HRE}. The purified protein sample was digested with 250 ng trypsin for overnight incubation at 37 °C. The resulting peptides were desalted using the C18 column, and the eluates were dried under a SpeedVac vacuum concentrator. Peptides were analyzed by LC-MS/MS using a Vanquish Neo UHPLC System coupled to an Orbitrap Eclipse Tribrid Mass Spectrometer with FAIMS Pro Duo interface (Thermo Fisher Scientific). The sample was loaded on a Neo trap cartridge coupled with an analytical column (75 μm ID × 50 cm PepMap™ Neo C18, 2 μm). Samples were separated using a linear gradient of solvent A (0.1% formic acid in water) and solvent B (0.1% formic acid in acetonitrile) over 120 min. For MS acquisition, FAIMS switched between CVs of −35 and −65 V with cycle times of 1.5 s per CV. MS1 spectra were acquired at 60,000 resolution with a scan range from 380 to 1400 m/z, normalized AGC target set at Standard mode, and maximum injection time set at Auto mode. Precursors were filtered using monoisotopic peak determination set to peptide, charge state 3 to 8, dynamic exclusion of 60 s with ±10 ppm tolerance. For the MS2 analysis, the isolated ions were fragmented by assisted higher-energy collisional dissociation (HCD) at 25 and 30% and acquired in an orbitrap at 30,000 resolution. The AGC and maximum IT were 200% and 70 ms, respectively.

The acquired MS/MS data was queried for disulfide cross-link identification against a target protein sequence using MeroX 2.0 software. The Disulfide bond was selected as the cross-linker, and the maximum number of missed cleavages was set to 4. The precursor mass tolerance was set to 20 ppm, and the fragment mass tolerance was set to 50 ppm. The search results were validated with 5% FDR and a precise scoring setting. The mass spectrometry proteomics data have been deposited to the ProteomeXchange Consortium via the PRIDE [1] partner repository with the dataset identifier PXD047859.

Thermal shift assay. The stability of each toxin variant was measured by quantifying the melting temperature of each toxin variant (50% denaturation point) compared to the wild-type toxin. Each well contained a final concentration of 5 μM protein and a 1:20 dilution of 5x Sypro Orange stock (Thermo Fisher S6650) in 20 mM Tris pH 7.5 and 150 mM NaCl buffer. The plates were heated in StepOnePlus™ Real-Time PCR System (Thermo Fisher) from 20 to 90 °C in increments of 0.3 °C. The wavelengths for excitation and emission were 490 and 575 nm, respectively.

Bacterial strains

S. aureus strains USA300/LAC, and the isogenic USA300/LAC Δ*hla* mutant were grown in tryptic soy broth (Bacto TSB, Fisher Scientific) overnight at 37 °C with agitation for 14–16 h. The Hla plasmid complemented *S. aureus* strain (Δ*hla::phla)* and the ovalbumin-expressing *S. aureus* strains were grown as described above with 20 μg/mL chloramphenicol selection. The strains were subcultured 1:100 in TSB the following day and grown to exponential phase (OD_{600} 0.5) and washed once with PBS, then resuspended in PBS to deliver 1×10^8 CFU in 50 μL via subcutaneous injection[15].

Plasmid construction for bacterial strains

The *hla* locus was deleted from the USA300 strain (Δ*hla)* using the pJB38 plasmid and the complemented strain (Δ*hla::phla)* was created with the pOS1 plasmid encoding *hla*, resulting in restoration of Hla expression[43]. A previously generated ovalbumin-expressing USA300 strain was utilized for the OT-II $CD4^+$ T cell subset analysis. In brief, this strain carries a plasmid engineered with an improved translation initiation region, optimized Shine-Dalgarno, and translation enhancer sequences, and an *S. aureus* codon-optimized chicken

egg ovalbumin sequence that includes the *S. aureus* Hla signal sequence for secretion[16].

Animal modeling

For all studies, animals were allocated randomly to experimental groups. Animals utilized for serum and tissue harvesting were randomly selected within each group. The Investigators were not blinded to allocation during experiments and outcome assessment.

Vaccine preparation and immunization. Vaccine antigens were LPS extracted and prepared as a 1:1 antigen to adjuvant formulation using the following: Alhydrogel 2% (InvivoGen, vac-alu-250), AddaS03 (InvivoGen, 10253-42-02), AS04-like formulation with antigen plus 500 μg/mL Alhydrogel 2% and 50 μg/mL of MPLA-SM (InvivoGen, vac-mpla), or CpG-ODN1585 (InvivoGen, 2 μg of CpG-ODN1585). For initial antigen screening and germinal center studies, 20 μg of each antigen was delivered via intramuscular (IM) injection to cohorts of 3-week-old or 5-week-old C57BL/6J male or female mice (offspring from C57BL/6 purchased from The Jackson Laboratory) on days 0 and 14. For the immunization of neonatal mice, 2 μg of each antigen was delivered in a total volume of 10μl IM to litters of C57BL/6 pups between P1-P3 with a boost delivered on P21 (day of weaning) with 50 μl total volume. Immunization of juvenile mice was conducted by delivery of 2 μg antigen in a total volume of 50 μl.

Skin and soft tissue infection modeling. All animal experiments were reviewed, approved, and supervised by the Institutional Animal Care and Use Committee (IACUC) at Washington University in St. Louis. To determine antibody titers, serum was collected from 5 to 10 mice per group, 1 week after boost immunizations and prior to the *S. aureus* challenge. C57BL/6 male and female mice 5–6 weeks of age were anesthetized via intraperitoneal injection of ketamine (20 mg/kg) and xylazine (5 mg/kg) followed by right flank subcutaneous challenge with 1×10^8 CFU *S. aureus* strain USA300/LAC in 50 μL PBS [71]. Lesional abscess and dermonecrosis area (mm^2) were measured at 24-h intervals for 10 days[44]. Abscesses were demarcated as the nodular and sometimes fluctuant area of subepithelial infection. Dermonecrosis area was measured independently as the area overlying the abscess where the epithelial injury was visible. Mice received a secondary infection on the left flank, 21–28 days after the start of the primary infection. Abscess and dermonecrosis size for all studies were determined according to the formula A = (π/2)(length mm)(width mm)[44]. All mice within each experiment were randomly selected for immunizations and age-matched.

Cell-based immunologic assays

Mass cytometry analysis. Ten days following either primary or secondary infection as indicated, the inguinal draining lymph node (dLN) was harvested from the ipsilateral side of *S. aureus* infected mice and processed to obtain single cell suspensions. A minimum of three dLN from independent mice were pooled together for each condition. Cells (3×10^6 per sample) were subjected to cisplatin labeling followed by staining for cell surface markers and intracellular antigens of interest with the antibody reagents, as noted in Supplementary Table 3. Fixation and cell permeabilization for intracellular staining were performed with the eBioscience Permeabilization Buffer and FoxP3 Transcription Factor Staining Buffer Set according to the manufacturer's protocol. Stained cells were washed, barcoded by sample, pooled, and analyzed on a Fluidigm CyTOF2 Helios mass cytometer by the Bursky Center for Human Immunology and Immunotherapy Programs at Washington University. De-barcoded samples were analyzed using Cytobank software (Beckman Coulter).

Flow cytometric analysis. Draining lymph nodes were processed as above to obtain a single-cell suspension. About 1×10^6 cells were then subjected to fluorescent antibody labeling, as noted in Supplementary Table 4 for extra- and intracellular staining. Viable cells were detected with Live/Dead Fixable Blue (Invitrogen L23105). Purified Hla antigen was labeled with Alexa Fluor 594 (Invitrogen A20104). These samples were run on a Cytek Aurora (spectral five lasers) and analyzed using Cytobank (Beckman Coulter).

Statistics and reproducibility

Sample sizes for each experiment were determined based on prior published data. The number of animals utilized in each experiment was based on the minimal number needed to achieve results of statistical significance. Statistical analysis for serologic studies and all in vitro assays was performed with GraphPad Prism 10 software using one-way ANOVA with Tukey's or Dunnette's multiple comparisons test or unpaired, two-tailed independent *t*-test. Assessment of statistical significance in skin infection studies was performed with GraphPad Prism 10 software using two-way ANOVA with Tukey's or Sidak's multiple comparisons test. Assessment of statistical significance in T cell analysis studies was performed with GraphPad Prism 10 software using either paired, two-tailed *T*-test or two-way ANOVA with Tukey's or Dunette's multiple comparisons test. Data results were considered statistically significant at a *P* value of 0.05 or less ($^*p < 0.05$, $^{**}p < 0.01$, $^{***}p < 0.001$, $^{****}p < 0.0001$). No data were excluded from the analysis except two male mice in Fig. 5g due to inconsistent hair growth cycle compared to other mice in group. All data is representative of at least two independent experiments. SDS-PAGE data are shown as representative gels of two independent experiments with similar results.

Reporting summary

Further information on research design is available in the Nature Portfolio Reporting Summary linked to this article.

Data availability

Data generated in this study are provided in the Source Data file. The mass spectrometry proteomics data in this study have been deposited in the ProteomeXchange Consortium via the PRIDE [1] partner repository which can be accessed at http://www.ebi.ac.uk/pride/archive/projects/PXD047859. A reporting summary is available for this study. Source data are provided with this paper.

References

1. Ikuta, K. S. Global mortality associated with 33 bacterial pathogens in 2019: a systematic analysis for the Global Burden of Disease Study 2019. *Lancet* **400**, 2221–2248 (2022).
2. Clegg, J. et al. *Staphylococcus aureus* vaccine research and development: the past, present and future, including novel therapeutic strategies. *Front. Immunol.* **12**, 705360 (2021).
3. Tsai, C. M. et al. Non-protective immune imprint underlies failure of *Staphylococcus aureus* IsdB vaccine. *Cell Host Microbe* **30**, 1163–1172.e1166 (2022).
4. Caldera, J. R. et al. The characteristics of pre-existing humoral imprint determine efficacy of *S. aureus* vaccines and support alternative vaccine approaches. *Cell Rep. Med.* **5**, 101360 (2024).
5. Berube, B. J. & Bubeck Wardenburg, J. *Staphylococcus aureus* alpha-toxin: nearly a century of intrigue. *Toxins* **5**, 1140–1166 (2013).
6. Wilke, G. A. & Bubeck Wardenburg, J. Role of a disintegrin and metalloprotease 10 in *Staphylococcus aureus* alpha-hemolysin-mediated cellular injury. *Proc. Natl Acad. Sci. USA* **107**, 13473–13478 (2010).
7. Inoshima, I. et al. A Staphylococcus aureus pore-forming toxin subverts the activity of ADAM10 to cause lethal infection in mice. *Nat. Med.* **17**, 1310–1314 (2011).

8. Inoshima, N., Wang, Y. & Bubeck Wardenburg, J. Genetic requirement for ADAM10 in severe Staphylococcus aureus skin infection. *J. Invest. Dermatol.* **132**, 1513–1516 (2012).
9. Powers, M. E., Kim, H. K., Wang, Y. & Bubeck Wardenburg, J. ADAM10 mediates vascular injury induced by Staphylococcus aureus alpha-hemolysin. *J. Infect. Dis.* **206**, 352–356 (2012).
10. Becker, R. E., Berube, B. J., Sampedro, G. R., DeDent, A. C. & Bubeck Wardenburg, J. Tissue-specific patterning of host innate immune responses by *Staphylococcus aureus* alpha-toxin. *J. Innate Immun.* **6**, 619–631 (2014).
11. Rosenbaum, D. & Saftig, P. New insights into the function and pathophysiology of the ectodomain sheddase A Disintegrin And Metalloproteinase 10 (ADAM10). *FEBS J.* **291**, 2733–2766 (2023).
12. Inoshima, N., Wang, Y. & Wardenburg, J. B. Genetic requirement for ADAM10 in severe *Staphylococcus aureus* skin infection. *J. Invest. Dermatol.* **132**, 1513–1516 (2012).
13. Powers, M. E., Becker, R. E., Sailer, A., Turner, J. R. & Bubeck Wardenburg, J. Synergistic action of *Staphylococcus aureus* alpha-toxin on platelets and myeloid lineage cells contributes to lethal sepsis. *Cell Host Microbe* **17**, 775–787 (2015).
14. Alfano, D. N., Miller, M. J. & Bubeck Wardenburg, J. Endothelial ADAM10 utilization defines a molecular pathway of vascular injury in mice with bacterial sepsis. *J. Clin. Invest.* **133**, e168450 (2023).
15. Sampedro, G. R. et al. Targeting Staphylococcus aureus alpha-toxin as a novel approach to reduce severity of recurrent skin and soft-tissue infections. *J. Infect. Dis.* **210**, 1012–1018 (2014).
16. Tkaczyk, C. et al. Identification of anti-alpha toxin monoclonal antibodies that reduce the severity of *Staphylococcus aureus* dermonecrosis and exhibit a correlation between affinity and potency. *Clin. Vaccin. Immunol.* **19**, 377–385 (2012).
17. Lee, B., Olaniyi, R., Kwiecinski, J. M. & Wardenburg, J. B. *Staphylococcus aureus* toxin suppresses antigen-specific T cell responses. *J. Clin. Invest.* **130**, 1122–1127 (2020).
18. Kleinhenz, M. et al. Toxin-neutralizing Abs are associated with improved T cell function following recovery from *Staphylococcus aureus* infection. *JCI Insight* **9**, e173526 (2024).
19. Fritz, S. A. et al. A serologic correlate of protective immunity against community-onset *Staphylococcus aureus* infection. *Clin. Infect. Dis.* **56**, 1554–1561 (2013).
20. Wu, Y. et al. Prevalence of IgG and neutralizing antibodies against *Staphylococcus aureus* alpha-toxin in healthy human subjects and diverse patient populations. *Infect. Immun.* **86**, e00671–17 (2018).
21. Hogan, P. G. et al. Impact of systemic antibiotics on *Staphylococcus aureus* colonization and recurrent skin infection. *Clin. Infect. Dis.* **66**, 191–197 (2018).
22. Menzies, B. E. & Kernodle, D. S. Site-directed mutagenesis of the alpha-toxin gene of *Staphylococcus aureus*: role of histidines in toxin activity in vitro and in a murine model. *Infect. Immun.* **62**, 1843–1847 (1994).
23. Sugawara, T. et al. Structural basis for pore-forming mechanism of staphylococcal alpha-hemolysin. *Toxicon* **108**, 226–231 (2015).
24. Walker, B. & Bayley, H. Key residues for membrane binding, oligomerization, and pore forming activity of staphylococcal alpha-hemolysin identified by cysteine scanning mutagenesis and targeted chemical modification. *J. Biol. Chem.* **270**, 23065–23071 (1995).
25. Ragle, B. E. & Bubeck Wardenburg, J. Anti-alpha-hemolysin monoclonal antibodies mediate protection against *Staphylococcus aureus* pneumonia. *Infect. Immun.* **77**, 2712–2718 (2009).
26. Pichichero, M. E. Challenges in vaccination of neonates, infants and young children. *Vaccine* **32**, 3886–3894 (2014).
27. Basha, S., Surendran, N. & Pichichero, M. Immune responses in neonates. *Expert Rev. Clin. Immunol.* **10**, 1171–1184 (2014).
28. Sakala, I. G., Eichinger, K. M. & Petrovsky, N. Neonatal vaccine effectiveness and the role of adjuvants. *Expert Rev. Clin. Immunol.* **15**, 869–878 (2019).
29. Victora, G. D. & Nussenzweig, M. C. Germinal centers. *Annu. Rev. Immunol.* **40**, 413–442 (2022).
30. Crotty, S. T follicular helper cell biology: a decade of discovery and diseases. *Immunity* **50**, 1132–1148 (2019).
31. Zhu, F. et al. Spatiotemporal resolution of germinal center Tfh cell differentiation and divergence from central memory CD4(+) T cell fate. *Nat. Commun.* **14**, 3611 (2023).
32. Fukuda, T. et al. Disruption of the Bcl6 gene results in an impaired germinal center formation. *J. Exp. Med.* **186**, 439–448 (1997).
33. Dan, J. M. et al. Recurrent group A *Streptococcus tonsillitis* is an immunosusceptibility disease involving antibody deficiency and aberrant T(FH) cells. *Sci. Transl. Med.* **11**, eaau3776 (2019).
34. Dan, J. M. et al. A cytokine-independent approach to identify antigen-specific human germinal center T follicular helper cells and rare antigen-specific CD4+ T cells in blood. *J. Immunol.* **197**, 983–993 (2016).
35. Vono, M. et al. Maternal antibodies inhibit neonatal and infant responses to vaccination by shaping the early-life B cell repertoire within germinal centers. *Cell Rep.* **28**, 1773–1784.e1775 (2019).
36. Ansell, D. M., Kloepper, J. E., Thomason, H. A., Paus, R. & Hardman, M. J. Exploring the "hair growth-wound healing connection": anagen phase promotes wound re-epithelialization. *J. Invest. Dermatol.* **131**, 518–528 (2011).
37. John, M. S. et al. Androgens at the skin surface regulate S. aureus pathogenesis through the activation of agr quorum sensing. Preprint at *bioRxiv* (2024).
38. Armentrout, E. I., Liu, G. Y. & Martins, G. A. T cell immunity and the quest for protective vaccines against *Staphylococcus aureus* infection. *Microorganisms* **8**, 1936 (2020).
39. Venkatasubramaniam, A. et al. Safety and immunogenicity of a 4-component toxoid-based *Staphylococcus aureus* vaccine in rhesus macaques. *Front. Immunol.* **12**, 621754 (2021).
40. Krishnaswamy, J. K., Alsen, S., Yrlid, U., Eisenbarth, S. C. & Williams, A. Determination of T follicular helper cell fate by dendritic cells. *Front. Immunol.* **9**, 2169 (2018).
41. McLellan, J. S. et al. Structure of RSV fusion glycoprotein trimer bound to a prefusion-specific neutralizing antibody. *Science* **340**, 1113–1117 (2013).
42. Simoes, E. A. F. et al. Prefusion F protein-based respiratory syncytial virus immunization in pregnancy. *N. Engl. J. Med.* **386**, 1615–1626 (2022).
43. Yang, F. et al. *Staphylococcus aureus* alpha-toxin impairs early neutrophil localization via electrogenic disruption of store-operated calcium entry. *Cell Rep.* **42**, 113394 (2023).
44. Bunce, C., Wheeler, L., Reed, G., Musser, J. & Barg, N. Murine model of cutaneous infection with gram-positive cocci. *Infect. Immun.* **60**, 2636–2640 (1992).

Acknowledgements

We thank Jacqueline Ansted and the Pediatric Sedation Service faculty and nurses at the University of Chicago for their support of pediatric clinical sample collections. This work was supported, in part, by the Bursky Center for Human Immunology and Immunotherapy Programs at Washington University, Immunomonitoring Laboratory. We thank Diane Bender, Roderick Lin, Olga Malkova, and Stephen Oh from the Bursky Center for support of Mass Cytometry Studies, Jaclyn Wright for insightful discussion on flow cytometric studies, and Lydia Wheat for review of the manuscript and editorial suggestions. This work was supported by NIH grants R01 AI097434 and R41 AI167137 (to J.B.W.) and R01 AI159677 and UL1RR024999 (to S.A.F. and J.B.W.).

Author contributions

K.L.T., R.O., S.A.F., and J.B.W. designed the studies. K.L.T., M.B., R.O., H.R.B., and J.B.W. performed a laboratory-based analysis of Hla vaccine

candidates, including all animal studies. H.R.B., S.H., A.C.D., S.A.F., and J.B.W. contributed to the collection, processing, and analysis of all human-derived samples. F.F., G.K.A., B-K.C., and Y.A.G. led studies to evaluate structural and biochemical attributes of the Hla antigens. K.L.T., R.O., S.A.F., and J.B.W. wrote the paper, which was reviewed and edited by all authors.

Competing interests

J.B.W. has a financial agreement with Aridis Pharmaceuticals related to patents owned by the University of Chicago. K.L.T., R.O., and J.B.W. may receive royalty income based on technology that is currently owned by Washington University and subject to licensing by Forward Defense, LLC. The remaining authors declare no competing interests.

Additional information

Supplementary information The online version contains supplementary material available at https://doi.org/10.1038/s41467-024-52714-7.

Correspondence and requests for materials should be addressed to Juliane Bubeck Wardenburg.

Peer review information *Nature Communications* thanks the anonymous reviewers for their contribution to the peer review of this work. A peer review file is available.